The Effect of Liposome Size on the Final Lipid/DNA Ratio of Cationic Lipoplexes

Elisabete Gonçalves,* Robert J. Debs,† and Timothy D. Heath*
*University of Wisconsin-Madison, School of Pharmacy, Madison, Wisconsin 53705; and †California Pacific Medical Research Center Institute, San Francisco, California 94115

ABSTRACT Several studies have demonstrated that lipoplexes are two-phase systems over most mixing lipid/DNA charge ratios. Because these studies have focused on small unilamellar vesicles (SUV), they leave open the question as to whether a similar pattern is followed by other liposome types. The main purpose of this work is to examine the question further by characterizing the assembly of cationic lipoplexes prepared from 1-[2-(oleoyloxy)ethyl]-2-oleyl-3-(2-hydroxyethyl)imidazolinium chloride (DOTIM)/dioleoylphosphatidylethanolamine (DOPE) (1:1) liposomes of various types. Sedimentation in sucrose density gradients reveals that large unilamellar vesicles (LUV) and sedimented multilamellar vesicles (sMLV), as opposed to SUV, form lipoplexes that exist as a single phase over a relatively broad range of mixing (+/−) ratios. This is indicated by observing that most of the LUV and sMLV become involved in the assembly reaction up to mixing (+/−) ratios of 4 and 9, respectively, while only a small and constant fraction of SUV associates with DNA at all mixing (+/−) ratios tested. Consequently, while maximal (+/−) ratios of ~4.5 and 9 are found in LUV and sMLV lipoplexes, respectively, a final (+/−) ratio of only ~2 is determined in SUV lipoplexes. Isothermal titration calorimetry shows that this is the lowest possible charge ratio achieved when liposomes are titrated with DNA. Based on these observations and on the size differences of the liposomes used, a model of lipoplex formation is proposed.

INTRODUCTION

Cationic lipid-DNA complexes, also known as lipoplexes (Felgner et al., 1997), have attracted much attention in recent years for their potential use in gene therapy. The absence of risk for infection, low immunogenicity, as well as ease of manufacturing and broad applicability makes lipoplexes a promising alternative to viral vectors. Currently, despite the large amount of research in lipoplex mediated gene transfection, the efficiency of these gene delivery systems is still lower than desirable.

A starting point to develop more efficient lipoplexes may be to acquire fundamental knowledge on lipoplex formation. Among the variety of physical interactions involved, electrostatic interactions are one of the most relevant. The concomitant release of condensed counterions into bulk solution, a phenomenon extensively studied in the context of other biomolecular association reactions (deHaseth et al., 1977; Mascotti and Lohman, 1990), has been experimentally observed upon lipoplex formation (Wagner et al., 2000; Simberg et al., 2001). The subsequent increase in entropy represents the major driving force for this reaction (Bruinsma, 1998; Harries et al., 1998), as it compensates for the positive enthalpy changes typically observed when pure cationic lipids interact with DNA (Spink and Chaires, 1997; Kennedy et al., 2000; Matulis et al., 2002; Pozharski and MacDonald, 2002).

DNA condensation and liposome restructuring are known to occur during lipoplex formation. Liposome restructuring involves both liposome fusion (Gershon et al., 1993; Mok and Cullis, 1997) and release of the vesicle aqueous contents (Kikuchi and Carmona-Ribeiro, 2000; Kennedy et al., 2000). Further evidence for liposome restructuring is provided from electron microscopy, which shows elongated rod-like structures (Gershon et al., 1993) and aggregates of globular particles (Sternberg et al., 1994; Mok and Cullis, 1997; Eastman et al., 1997). Cryoelectron microscopy (Gustafsson et al., 1995; Lasic et al., 1997; Huebner et al., 1999; Schmutz et al., 1999) and small angle x-ray scattering studies of such aggregates (Lasic et al., 1997; Rädler et al., 1997; Boukhnikachvili et al., 1997) reveal an internal multilamellar structure, where lipid bilayers alternate with hydrated DNA monolayers. This lamellar structure coexists with an inverted hexagonal structure when the cationic liposomes contain dioleoylphosphatidylethanolamine (DOPE) at molar ratios greater than 0.41 (Koltover et al., 1998; Lin et al., 2000).

Lipoplexes prepared from small unilamellar vesicles (SUV) are commonly found in coexistence with a second phase, either cationic liposomes or DNA, depending on whether their preparation takes place above or below a (+/−) ratio of 1, respectively (Rädler et al., 1997, 1998; Xu et al., 1999). Separation of the excess component by sedimentation in sucrose density gradients followed by analysis of the lipid and DNA content of the purified lipoplexes shows that the final lipid/DNA ratios are constant in each regime, with (+/−) ratios of ~0.5 and 3 for lipoplexes prepared below and above a (+/−) ratio of 1, respectively (Xu et al., 1999).

Submitted July 10, 2003, and accepted for publication November 10, 2003.

Address reprint requests to Timothy D. Heath, University of Wisconsin-Madison, School of Pharmacy, 777 Highland Ave., Madison, WI 53705. E-mail: tdheath@pharmacy.wisc.edu.

Elisabete Gonçalves' present address is Dept. of Biophysical Chemistry, Biozentrum, University of Basel, Klingelbergstrasse, 70, CH-4056, Basel, Switzerland.

0006-3495/04/03/1554/10 $2.00

Similarly to the study of Xu and co-workers, this work characterizes lipoplex formation by determining the final lipid/DNA ratios of lipoplexes. Focusing on the excess cationic lipid regime, the main question addressed here is whether the type of liposomes used in lipoplex formation affects the fraction of lipid that binds to DNA. We were prompted to pursue this question because of an electron microscopy study done by our group showing a larger fraction of DNA-free liposomes when SUV are used to complex DNA instead of sedimented multilamellar vesicles (sMLV) (Jang and Heath, 1997). Additional motivation for this study came from the lack of characterization studies using MLV lipoplexes, and from the well established knowledge that these are better transfecting agents than SUV lipoplexes (Felgner et al., 1994; Liu et al., 1997; Ross et al., 1998; MacDonald et al., 1999; Ross and Hui, 1999; Zuidam et al., 1999), thus making their characterization an essential step toward the development of more efficient gene delivery systems.

Using three types of 1-[2-(oleoyloxy)ethyl]-2-oleyl-3-(2-hydroxyethyl)imidazolinium chloride (DOTIM)/DOPE (1:1) liposomes, with diameters varying from 25 nm up to >1 μm, and a 7.2-kb plasmid, we present an extensive characterization of the effect of liposome type on lipoplex formation. In addition to the sedimentation studies, the association reaction is also characterized using isothermal titration calorimetry. A model is proposed to explain the results obtained.

MATERIALS AND METHODS

Materials

Chemicals

DOPE and *N*-(lissamine rhodamine B sulfonyl)phosphatidylethanolamine (*N*-Rh-PE) were obtained from Avanti Polar Lipids (Alabaster, AL). The cationic lipid DOTIM was synthesized as previously described (Solodin et al., 1995). All lipids were dissolved in chloroform and stored under argon at −20°C. Sodium deoxycholate and Hepes were purchased from Sigma (St. Louis, MO) and sucrose was obtained from Mallinckrodt (St. Louis, MO). Glucose was from Fisher Scientific (Fair Lawn, NJ).

Plasmid DNA

p4241, a 7.2-kb plasmid expressing the luciferase gene, was isolated and purified as previously described (Liu et al., 1997). DNA concentration in the stock solutions was determined spectroscopically assuming an absorbance of 1 at 260 nm for a 50-μg/ml solution (0.15 mM DNA phosphate). The A_{260}/A_{280} was always between 1.8 and 1.9, indicating that there was no protein or RNA contamination.

Liposome and lipoplex preparation

MLV were prepared from 49.75:49.75:0.5 DOTIM/DOPE/*N*-Rh-PE in a screw-capped glass tube, protected from light. Chloroform was removed in a rotary evaporator, and the thin lipid film was then exposed to a vacuum overnight. The lipids were resuspended in nonionic aqueous media (water or 5% w/v glucose), with gentle vortex mixing, and further incubated at 45°C, for ~6 h, to give a milky suspension of MLV. SUV were produced by sonication of MLV, usually for 20 min, in a cylindrical sonic bath (Laboratory Supplies, Hicksville, NY) until a translucent lipid suspension was obtained. Large unilamellar vesicles (LUV) were prepared by extrusion of MLV suspensions in an extruder (Lipex Biomembranes, Vancouver, Canada) attached to an argon cylinder. The MLV were extruded six times at moderate pressure (<2000 kPa) through two stacked 13-mm polycarbonate membranes with pore diameters of 50 nm, 100 nm, or 200 nm, depending on the intended vesicle size. Sedimentation of an aqueous suspension of MLV at 85,000 $\times$ *g* for 45 min at 10°C, in a Beckman L8-60M Ultracentrifuge equipped with a SW 55Ti rotor (Beckman Coulter, Fullerton, CA) produced a thick pellet of sMLV, which was resuspended in water after carefully removing the supernatant. The DOTIM concentration in the liposome suspensions was typically 10 mM, and was measured from the absorbance at 238 nm, using a molar extinction coefficient for DOTIM of 6809.2 $M^{-1}cm^{-1}$.

Stock suspensions of liposomes and DNA were diluted in Hepes buffer (Hepes 10 mM, NaCl 10 mM, pH 7.4) before lipoplex formation, which was achieved by adding 1 vol diluted plasmid DNA to 3 vol diluted liposome suspension (SUV, LUV, or sMLV), with gentle mixing. The final concentration of DOTIM in the lipoplexes was usually 0.625 mM and the DNA concentration varied between 62.5 and 25 μg/ml depending on the mixing (+/−) ratios. DOTIM and DNA content of lipoplexes was checked after their formation using the quantification procedures described below.

Transmission electron microscopy

Samples were prepared for transmission electron microscopy by negative staining with uranyl acetate using a two-step method. A drop of liposome suspension was first applied onto a pioloform (Ted Pella, Redding, CA) coated 400 mesh Ni thin bar grid, allowed to adsorb for 1 min, and then blotted with filter paper. After air-drying for 3 min, a drop of 2% aqueous uranyl acetate stain was applied to the prepared sample grid and immediately blotted with filter paper. In the case of sMLV, resolution was improved with fixation by combining and vortexing (10 s) the sMLV suspension with an equal volume of 1% osmium tetroxide. Total osmium tetroxide fixation time was 1 min at room temperature. Then, the osmium/sample solution was placed on the pioloform grid and stained with uranyl acetate as described above. After the negatively stained samples air-dried for 3 min, they were examined on a Philips CM120 TEM at 80 kV (Philips Electron Optics, Eindhoven, The Netherlands).

Dynamic light scattering

Particle size was measured at 20°C, in a Nicomp 380 ZLS dynamic light scattering instrument (Nicomp Particle Sizing Systems, Santa Barbara, CA), equipped with a 30-mW laser (632.8-nm wavelength) and an Avalanche photodiode detector. The scattered light intensity detected at a 90° angle was treated using the Gaussian or multimodal Nicomp analysis, depending on the polydispersity of the samples, and the data presented corresponds to the volume weighted distributions. The mean diameters shown are averages of 3–6 measurements performed on different samples for periods of time long enough (from 15 min to 24 h) to collect statistically reliable data.

Discontinuous sucrose density gradients

After 30-min incubation the lipoplexes were characterized by sedimentation to equilibrium in discontinuous sucrose density gradients. The gradients were prepared in 13- × 51-mm Ultra-Clear centrifuge tubes by successively layering 2 ml 20%, 1 ml 10%, and 1 ml 5% w/v sucrose. The lipoplex suspension was then loaded on the top of the gradient and sedimented at 116,000 $\times$ *g* for 16 h at 10°C, in a Beckman L8-60M Ultracentrifuge, equipped with a SW 55Ti rotor (Beckman Coulter). Gradients were fractionated after sedimentation based on the position of the lipoplex bands.

The position of each fraction in the gradient was expressed by determining its cumulative volume, calculated by adding half the fraction volume to the volume of any fractions located above it. Each fraction was assayed for both DOTIM and DNA content using the procedures described below.

DOTIM and DNA quantification

The DOTIM concentration was determined after sodium deoxycholate (12 mM) solubilization of the complexes by measurement of *N*-Rh-PE fluorescence intensity at 590 nm, with an excitation wavelength of 550 nm (slit widths of 5 nm), in a Hitachi F-3010 fluorescence spectrophotometer (Hitachi Instruments, San Jose, CA). The DNA concentration in each fraction was determined both by UV spectroscopy and fluorimetry. In the UV spectroscopic assay, the material present in each fraction was solubilized in sodium deoxycholate (12 mM), and the absorbance at 275 nm was measured using a Hitachi-3000 UV/VIS spectrophotometer (Hitachi Instruments). Owing to the absorbance of DOTIM and *N*-Rh-PE at 275 nm, it was necessary to correct the DNA absorbance readings of the complexes by first subtracting the contribution of these two components for the absorbance reading. The contribution of DOTIM and *N*-Rh-PE to the absorbance was determined by using a standard curve where fluorescence intensities of *N*-Rh-PE at 590 nm were correlated to the absorbance of both components at 275 nm. After this correction, DNA concentration was calculated using a DNA standard curve. In the fluorimetric assay, lipoplexes were extracted with chloroform and methanol (Bligh and Dyer, 1959) to remove lipid, Hoechst dye ([Hoechst] = 0.4 μg/ml) was added to the aqueous phase, and the fluorescence signal of the DNA-Hoechst dye complex was followed at 465 nm, with excitation at 350 nm (slit widths of 5 nm), using the fluorescence spectrophotometer mentioned above. No DNA was detected in the chloroform phase of the extraction. The final DNA concentrations were calculated from a standard curve obtained after chloroform/methanol extraction of DNA standard solutions.

Isothermal titration calorimetry

The enthalpy change associated with the interaction between DOTIM/DOPE (1:1) liposomes and plasmid DNA was measured using an isothermal titration calorimeter (MicroCal, Northampton, MA) at 25°C. Before the measurements, both plasmid DNA (7.2 kb) and liposomes (SUV or sMLV) were extensively dialyzed against Hepes buffer (10 mM Hepes, 10 mM NaCl, pH 7.4) and degassed for 15 min. Approximately 1.7 ml of a sample consisting of DOTIM/DOPE (1:1) liposomes was loaded into the sample cell (vol = 1.338 ml) and 10-μl aliquots of DNA solution were injected into the cell using the automated 250-μl rotating stirrer-syringe at constant time intervals of 6 min. Similar results were obtained using concentrations of 0.4 mM DOTIM and 3 mM DNA phosphate groups or 0.2 mM DOTIM and 1.5 mM DNA, respectively. A control titration, in which DNA was added to pure buffer, was used to correct the enthalpy of each injection for the heat of DNA dilution. Raw data were processed using Origin graphing software provided with the instrument.

RESULTS

Particle size analysis of liposomes

Table 1 shows the mean diameters of DOTIM/DOPE (1:1) liposomes. SUV have a mean volume-weighted diameter of 47.2 nm, whereas for sMLV the value is 850 nm. Particle size distributions (Fig. 1 *c*) show SUV and sMLV to be polydisperse. For the SUV, the majority of vesicles are 25 nm in diameter, with a smaller fraction of vesicles close to 100 nm, whereas for the sMLV most vesicles are close to 1 μm in diameter, with a smaller fraction of vesicles in the 300-nm range. These size measurements were confirmed by negative staining transmission electron microscopy, which shows a large fraction of SUV 25–30 nm in diameter (Fig. 1 *a*), whereas sMLV suspensions contain vesicles whose diameters vary from 500 nm to almost 2 μm (Fig. 1 *b*). LUV extruded to 50, 100, and 200 nm have mean diameters of 75.9, 127.7, and 180.0 nm, respectively (Table 1). Of the three LUV preparations, the 50-nm extruded vesicles are the most homogeneous, as indicated by the narrower peak distributions (Fig. 1 *d*).

TABLE 1 Characterization of DOTIM/DOPE (1:1) liposomes using dynamic light scattering

Liposome type	Mean diameter ± SD, nm
SUV	47.2 ± 32.4
LUV 50	75.9 ± 25.5
LUV 100	127.7 ± 88.6
LUV 200	180.0 ± 98.3
sMLV	854 ± 390

The mean diameters and standard deviations (SD) of the particle size distributions shown are averages of 3–6 measurements performed on different liposome preparations for periods of time ranging from 15 min up to 24 h.

Final lipid/DNA ratios of sedimented lipoplexes

SUV and sMLV

Fig. 2 shows the discontinuous sucrose density gradients obtained with DOTIM/DOPE (1:1) SUV and sMLV lipoplexes prepared at a (+/−) ratio of 3.6. The SUV gradient contains a translucent band on the top, and a denser, more turbid band, located at the interface between the 10 and 20% w/v sucrose layers. The sMLV lipoplex gradient shows no evidence of a lipid band on the top, and contains one band at the interface of the 10 and 20% w/v sucrose layers, and a more diffuse band within the 10% w/v sucrose layer. Therefore, as shown in earlier microscopy studies (Jang and Heath, 1997), these results point to the existence of a larger amount of free liposomes in DOTIM/DOPE (1:1) SUV lipoplex suspensions as compared to sMLV lipoplexes. Quantification of DOTIM and DNA in the gradient fractions, shown in Table 2, confirmed this observation. Approximately one third of the DOTIM in SUV lipoplexes is located in fractions 1 and 2, whereas only 5.5% of the DOTIM is found at a similar position (fraction 1) for sMLV lipoplexes. The negligible amounts of DNA found in these fractions for both lipoplex types confirm that this lipid corresponds to free liposomes. Most of the DNA (~73%) in SUV lipoplexes is detected in fraction 4, whereas for sMLV lipoplexes the DNA distributes mainly between fractions 3 and 4, most being found in the lower density fraction 3. The difference between SUV and sMLV lipoplexes described above is accurately reflected in the weighted average final (+/−) ratios, which we have calculated for all fractions containing significant amounts of

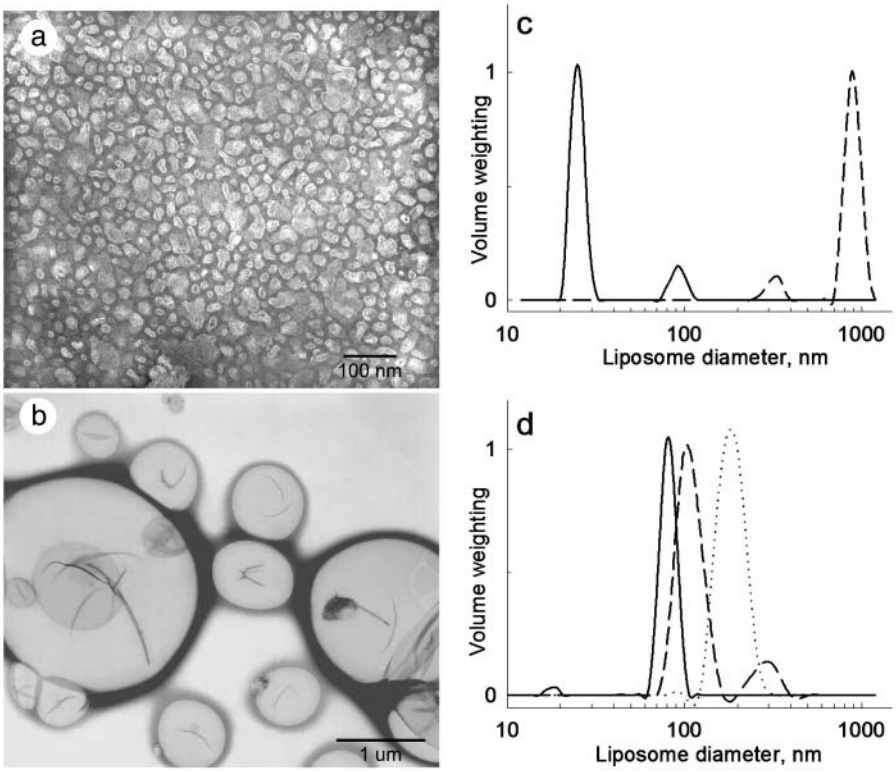

FIGURE 1 Particle size of liposomes. (*a* and *b*) Transmission electron micrographs of DOTIM/DOPE (1:1) SUV (*a*) and sMLV (*b*) obtained after negative staining with uranyl acetate. The sMLV samples were fixed with osmium tetroxide before staining with uranyl acetate. (*c*) Volume-weighted Nicomp (multimodal) particle size distributions from dynamic light scattering of DOTIM/DOPE (1:1) SUV (*solid line*) and sMLV (*dashed line*). (*d*) Volume-weighted Gaussian particle size distributions of LUV extruded through polycarbonate membranes with pore diameters of 50 (*solid line*), 100 (*dashed line*), or 200 nm (*dotted line*).

both lipid and DNA (3 and 4 for SUV and 2–4 for sMLV lipoplexes). This value is 3.4 for sMLV lipoplexes, but only 2.1 for SUV lipoplexes. The weighted average final (+/−) ratios are used in the studies described below.

Fig. 3 shows the DOTIM and DNA sedimentation profiles of lipoplexes prepared from DOTIM/DOPE (1:1) SUV and sMLV at various mixing (+/−) ratios. For the SUV lipoplexes, the distribution profiles are similar for all mixing ratios used, with a major fraction of DNA and some DOTIM sedimenting to ~2.5 ml from the top of the gradient. There is also an increasing accumulation of DOTIM in the first two gradient fractions as the mixing (+/−) ratios are increased. This lipid is identified as DNA-free liposomes, not only because SUV tend to accumulate at this position when sedimented in the absence of DNA (SUV curve), but also because insignificant amounts of DNA are found in these fractions at all mixing (+/−) ratios.

For sMLV lipoplexes, both DOTIM and DNA accumulate at ~1.6 ml from the gradient top for lower mixing (+/−) ratios (≤4.2), but are progressively displaced to ~0.7 ml from the gradient top at higher mixing (+/−) ratios. The amount of lipid retained in the first gradient fraction increases slightly upon increase of the mixing (+/−) ratios. sMLV sedimented in the absence of DNA (sMLV curve) are also found in fraction 1, confirming that the lipid retained in this fraction corresponds to DNA-free liposomes.

The final (+/−) ratios are plotted as a function of the mixing (+/−) ratios in Fig. 4. Lipoplexes made from SUV show a constant final (+/−) ratio of ~2, regardless of the mixing ratios used in lipoplex formation. In contrast, sMLV form lipoplexes whose final (+/−) ratios increase in direct proportion to the initial mixing (+/−) ratios, showing an almost quantitative incorporation of the cationic lipid into the lipoplexes.

LUV

Fig. 5 shows the DOTIM and DNA sedimentation profiles obtained for lipoplexes prepared from three different LUV

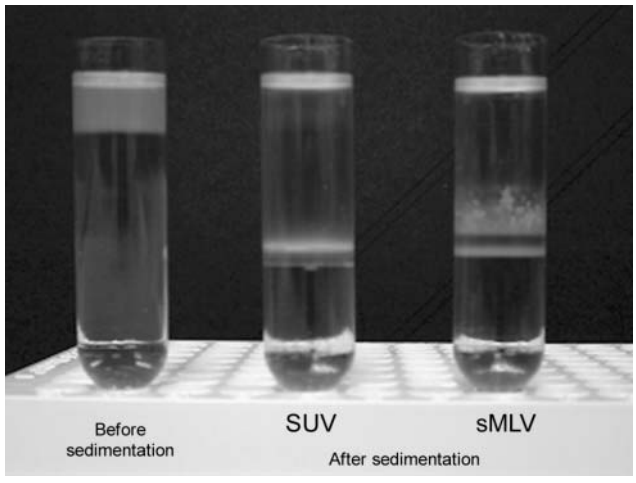

FIGURE 2 Sedimentation of DOTIM/DOPE (1:1) lipoplexes in discontinuous sucrose density gradients. Cationic lipoplexes were prepared from either SUV or sMLV at a (+/−) ratio of 3.6 and sedimented at 116,000 × *g* for 16 h, at 10°C, in discontinuous sucrose density gradients.

TABLE 2 Composition of lipoplexes prepared from DOTIM/DOPE (1:1) liposomes after sedimentation in sucrose density gradients

Lipoplex	Mixing ratio (+/−)	Fraction	Cumulative volume, ml	DOTIM (% of total)	DNA (% of total)	Final ratio* (+/−)
SUV	3.6 ± 0.2	1	0.13 ± 0.02	16.3 ± 1.8	0.9 ± 0.3	2.1 ± 0.08
		2	0.42 ± 0.03	15.2 ± 0.8	1.4 ± 0.3	
		3	1.35 ± 0.03	11.8 ± 3.3	16.7 ± 4.1	
		4	2.45 ± 0.08	41.0 ± 2.8	72.6 ± 1.5	
sMLV	3.8 ± 0.5	1	0.15 ± 0.01	5.5 ± 0.8	1.2 ± 0.2	3.4 ± 0.33
		2	0.69 ± 0.02	11.8 ± 4.4	5.3 ± 2.4	
		3	1.55 ± 0.03	45.5 ± 5.7	49.9 ± 5.0	
		4	2.32 ± 0.07	20.1 ± 2.1	31.7 ± 4.7	

Cationic lipoplexes were prepared from either SUV or sMLV at the (+/−) ratios indicated in the table, and sedimented at 116,000 × *g* for 16 h, at 10°C. After sedimentation, the gradient was fractionated by collecting fractions from the top of the tubes, and the volume of each fraction was recorded. DOTIM and DNA content was determined in each fraction as described under Materials and Methods. Results are mean values of three determinations ± standard deviations. The total recovery of DOTIM and DNA in all the fractions was usually >85%.

*(+/−) ratios were calculated taking into consideration that 1 nmol DOTIM contains 1 nmol positive charge and 1 μg DNA is 3 nmol negatively charged phosphate.

preparations described above (Table 1; Fig. 1). LUV lipoplexes sediment to ~2 ml from the gradient top at the lowest mixing (+/−) ratios, and are progressively displaced toward lower density positions at higher mixing (+/−) ratios. The final (+/−) ratios obtained from these studies are plotted against the mixing (+/−) ratios in Fig. 6. All three LUV preparations form lipoplexes for which the final (+/−) ratio appears to approach a maximum of 4.5–5, and is close to the mixing ratio for (+/−) ratios below ~4. No significant differences in the final (+/−) ratios are observed among the three types of LUV lipoplexes.

Particle size analysis of sedimented lipoplexes

Fig. 7 shows the particle size for a series of SUV and sMLV lipoplex preparations sedimented in sucrose density gradients. The results shown are the mean volume-weighted diameters of the lipoplexes isolated in fraction 4 for SUV

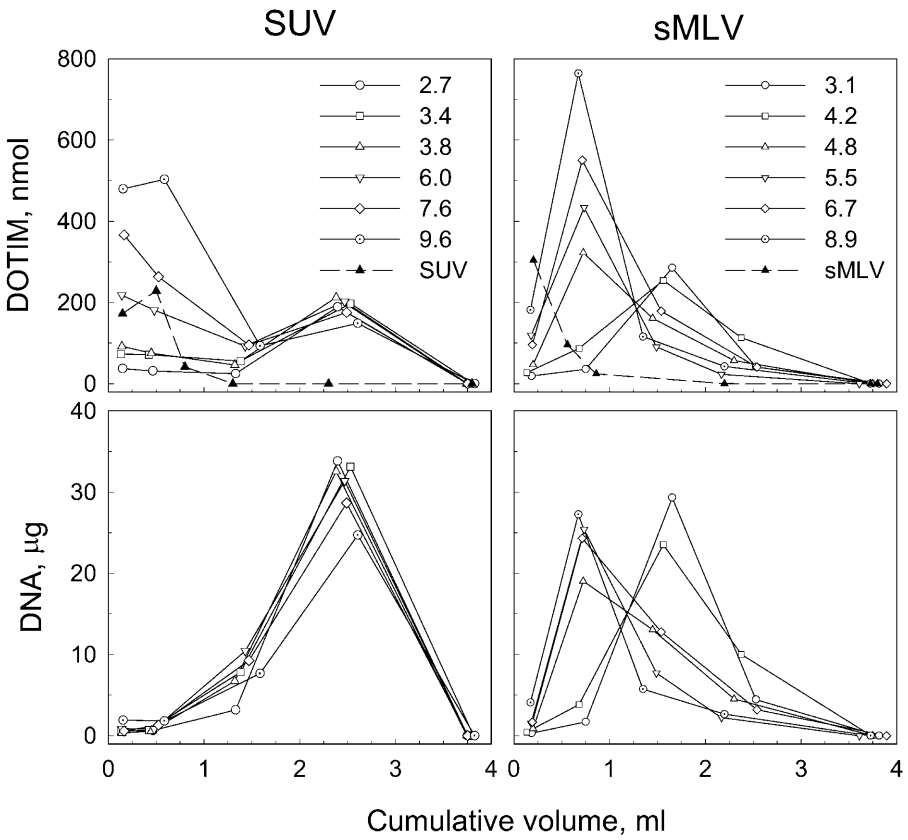

FIGURE 3 DOTIM and DNA sedimentation profiles of lipoplexes prepared from a 7.2-kb plasmid and DOTIM/DOPE (1:1) SUV or sMLV. The results shown are the amounts of DOTIM and DNA detected in each fraction collected from the gradient. The cumulative volume indicates the position of each fraction in the gradient, and the mixing (+/−) ratio used in lipoplex formation is indicated in the legends. The SUV and sMLV curves correspond to the sedimentation of DNA-free liposomes.

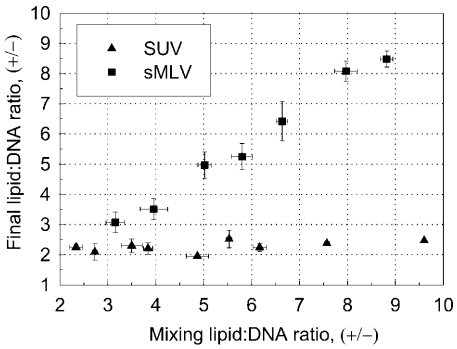

FIGURE 4 Final (+/−) ratios in lipoplexes prepared from a 7.2-kb plasmid and DOTIM/DOPE (1:1) SUV or sMLV. Cationic lipoplexes were prepared from each liposome type at various (+/−) ratios and sedimented in discontinuous sucrose density gradients. The final (+/−) ratios were calculated from the DNA and DOTIM content of fractions 3 and 4 for SUV lipoplexes, and fractions 2, 3, and 4 for sMLV lipoplexes. There are 4–6 replicates in each point.

lipoplexes, and in fraction 3 for sMLV lipoplexes. Sedimented SUV lipoplexes have a mean diameter of 201.2 nm at a mixing (+/−) ratio of 2.7, which is ~8 times larger than the original size of most SUV (Fig. 1). The limited reduction in lipoplex size observed upon increase of the mixing (+/−) ratios suggests that SUV lipoplexes are constant in size. sMLV lipoplexes have a mean diameter of ~850 nm for the range of mixing (+/−) ratios tested, which is similar to the mean diameter found in the DNA-free sMLV (Table 1). A small decrease in lipoplex size is observed upon increase of the mixing (+/−) ratios.

Enthalpy changes associated with DOTIM/DOPE (1:1) liposome-DNA interactions

The association reaction between DOTIM/DOPE (1:1) liposomes and DNA was characterized by isothermal titration calorimetry. Fig. 8 *a* shows typical calorimetric traces obtained after addition of successive amounts of DNA to buffer, SUV, or sMLV, and Fig. 8 *b* represents the cumulative heat curves plotted against the (−/+) ratios for each liposome type. The enthalpy change detected upon interaction between DOTIM/DOPE (1:1) liposomes and DNA is negative, revealing that lipoplex formation occurs through an exothermic reaction. The endpoints of the SUV and sMLV titrations are separated by only one DNA injection, showing that the reaction progresses to the same extent for both liposome types. The endpoints occur at (−/+) ratios of 0.5 for SUV and 0.45 for sMLV, which correspond to (+/−) ratios of 2.0 and 2.2 for SUV and sMLV, respectively.

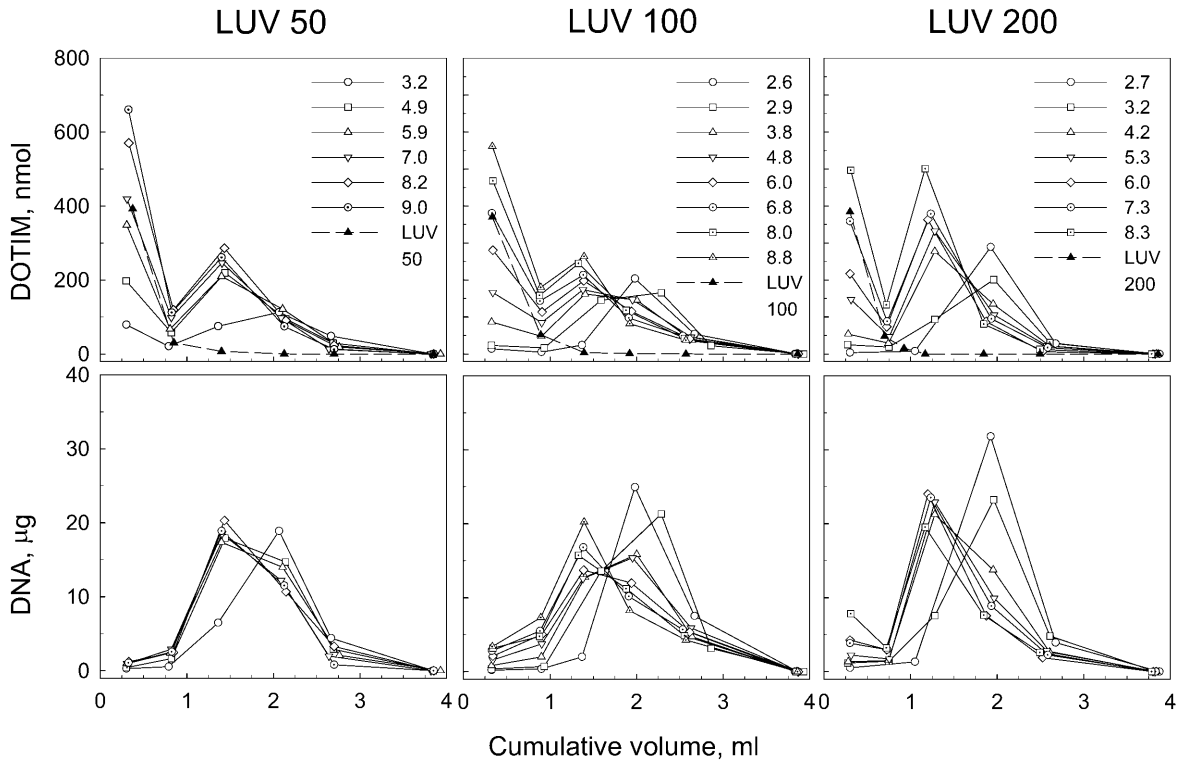

FIGURE 5 DOTIM and DNA sedimentation profiles of lipoplexes prepared from a 7.2-kb plasmid and DOTIM/DOPE (1:1) LUV extruded through membranes with pore diameters of 50 (LUV 50), 100 (LUV 100), and 200 nm (LUV 200). The numbers in the legends indicate the (+/−) ratios used in lipoplex formation. The LUV curves (LUV 50, 100, and 200) correspond to the sedimentation of DNA-free LUV.

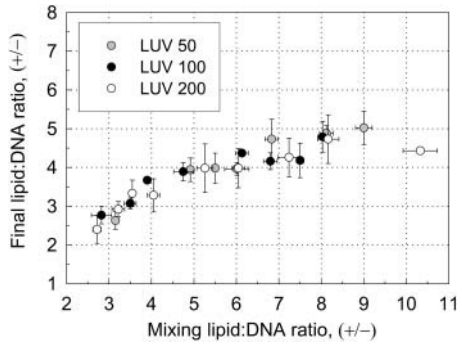

FIGURE 6 Final (+/−) ratios in lipoplexes prepared from a 7.2-kb plasmid and DOTIM/DOPE (1:1) LUV obtained by extrusion through polycarbonate membranes with pore diameters of 50 (LUV 50), 100 (LUV 100), and 200 nm (LUV 200). All fractions, except fraction one, were considered in the calculation of the final lipid/DNA ratios. There are 4–6 replicates in each point.

DISCUSSION

The most striking observation made in this study is that lipoplexes can exist as single-phase systems over a much broader range of mixing lipid/DNA ratios than previously reported. Focusing on the excess cationic lipid regime, we show that this is the case with sMLV and the three LUV lipoplex preparations analyzed. This conclusion is based on the relatively small amounts of DNA-free liposomes found in sMLV lipoplexes up to mixing (+/−) ratios close to 9 (Fig. 3), and by observing a similar trend in LUV lipoplexes prepared at (+/−) ratios below ~4 (Fig. 5). In agreement with previous studies (Rädler et al., 1997, 1998; Xu et al., 1999), and contrasting with the other two lipoplex types, SUV lipoplexes coexist with a significant excess of liposomes at most of the mixing (+/−) ratios tested (Fig. 3). Stating the situation differently, significantly higher final (+/−) ratios may be achieved when lipoplexes are prepared from larger liposomes. This is clearly illustrated by comparing the (+/−) ratio of ~2 found in the isolated SUV lipoplexes (Fig. 4) with the maximal values of ~4.5 and 9 found in the LUV (Fig. 6) and sMLV lipoplexes (Fig. 4), respectively. Because sMLV do not appear to reach a saturating final (+/−) ratio within the range of mixing ratios tested (Fig. 4), it is possible that a bigger difference separates sMLV from the other two types of lipoplexes.

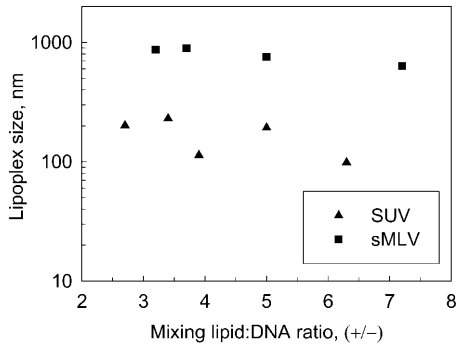

FIGURE 7 Mean particle size of SUV lipoplexes sedimented in fraction 4 and sMLV lipoplexes sedimented in fraction 3 as a function of the mixing lipid/DNA ratios. The values shown are the volume-weighted mean diameters of the Gaussian distributions.

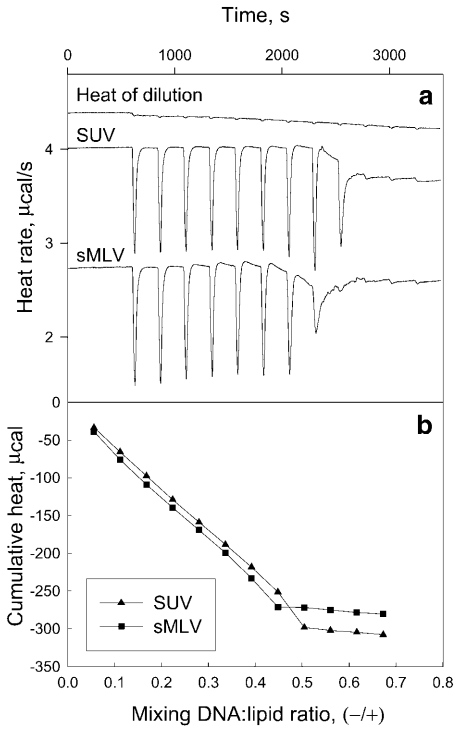

FIGURE 8 (*a*) Isothermal titration calorimetric traces and (*b*) cumulative heats of reaction obtained after titration of DOTIM/DOPE (1:1) SUV or sMLV (0.4 mM in DOTIM) with 10-μl aliquots of a 7.2-kb plasmid (3 mM), at 25°C. The heat of dilution was obtained by titrating DNA into pure buffer (10 mM Hepes, 10 mM NaCl, pH 7.4). A quantity of 30 nmol DNA was added in each injection, and the calorimeter cell contained a total of 535 nmol DOTIM.

MLV lipoplexes are generally better transfecting agents than SUV lipoplexes (Felgner et al., 1994; Liu et al., 1997; Ross et al., 1998; MacDonald et al., 1999; Ross and Hui, 1999; Zuidam et al., 1999). The larger size of MLV lipoplexes, often indicated as the main reason, might not be the only factor involved, since these are still better transfecting vectors than SUV lipoplexes of comparable size (Ross and Hui, 1999). The absolute requirement of an excess of cationic lipid for efficient gene transfection (Barron et al., 1999), suggests that the higher final (+/−) lipoplex ratios achieved with larger liposomes may correlate in some way with higher gene expression levels. This hypothesis is currently under analysis.

The effect of liposome size on lipoplex formation is of considerable significance, and we may explain this effect by constructing a model of what happens when DNA first binds to the liposomes during lipoplex formation (Fig. 9). Theoretical estimates show that our dominant SUV population (25 nm in diameter) contains ~2000 cationic lipid

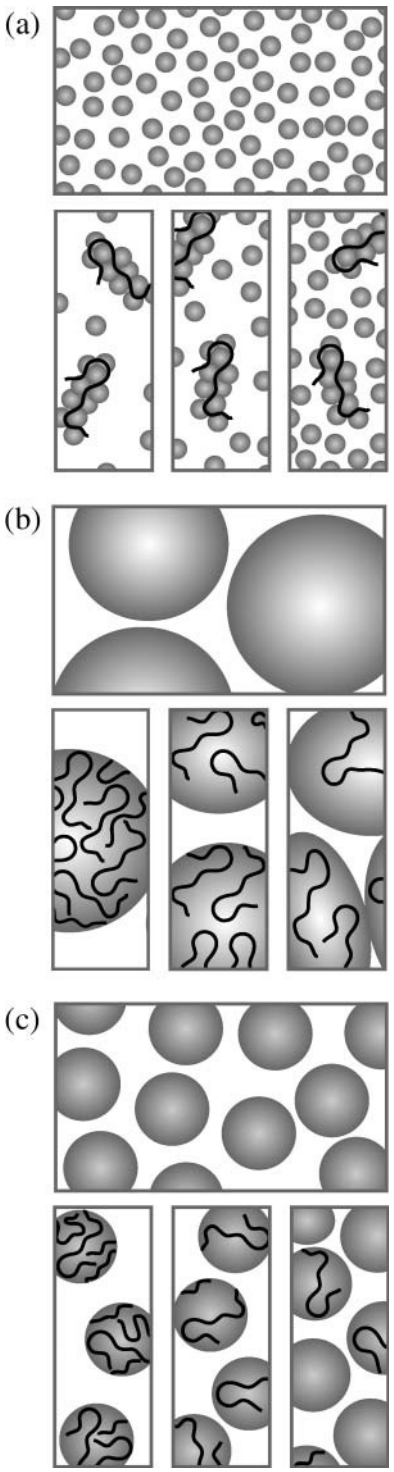

FIGURE 9 Schematic model of lipoplex formation when a 7.2-kb plasmid is mixed with (*a*) SUV, (*b*) sMLV, and (*c*) LUV. The top panels represent the liposome preparations (*spheres*) before adding the plasmid (*wavy solid line*), and the bottom panels represent the lipoplexes formed at an excess of cationic lipid. In each case, the mixing (+/−) ratios increase from left to right.

molecules per vesicle, as compared to 14,400 anionic phosphate charges present in the 7.2-kb plasmid. (The number of cationic lipid molecules in the lipid bilayer was estimated assuming that liposomes are hollow spheres of the indicated diameter (d), that the cross-sectional area of each lipid molecule is 0.7 nm^2, and that the bilayer is 4-nm thick. The surface area of the internal and external monolayers was calculated using the formula $A = 8\pi(0.25d^2 - 2d + 8)$, and the value thereby obtained was divided by 2×0.7, to account for the presence of 50 mol% neutral lipid (e.g., DOPE) in the vesicles.) Therefore, for SUV lipoplexes prepared at an excess of cationic lipid, multiple liposomes will initially associate with each 7.2-kb plasmid in solution (Fig. 9 *a*). The association of SUV with DNA will occur only until a slight excess of cationic lipid is incorporated into the complexes. Subsequently, liposomes and DNA should rearrange into a condensed phase as shown by others (Gershon et al., 1993; Mok and Cullis, 1997), but electrostatic repulsions should prevent further binding of SUV to the positively charged complexes. Therefore, SUV lipoplexes are predicted by our model, as observed here and elsewhere, to have relatively constant and small final (+/−) ratios (Fig. 4), and to coexist with an excess of cationic liposomes at most mixing (+/−) ratios above charge neutrality (Fig. 3). The significant increase in particle size observed upon lipoplex formation (Fig. 7) is also in agreement with the involvement of multiple SUV, suggesting extensive liposome fusion, as shown by others (Gershon et al., 1993; Mok and Cullis, 1997).

In regard to sMLV lipoplexes (Fig. 9 *b*), a very different situation exists. A 900-nm unilamellar vesicle, the average size of our sMLV, contains 3.6×10^6 cationic lipid molecules, which is sufficient to neutralize 250 molecules of the 7.2-kb plasmid. There will be an average of ~23 plasmids present per sMLV at a mixing (+/−) ratio of 10, which is the highest ratio we have used. Since the number of plasmids per liposome is inversely related to the mixing (+/−) ratio, 23 is the smallest number of plasmids per sMLV in our studies. Therefore, all liposomes are certain to interact with DNA, because there are at least 23 plasmids present per liposome. Furthermore, the average number of DNA molecules binding initially to each sMLV can change and, therefore, will decrease upon increase of the mixing (+/−) ratio. As a consequence, and consistent with the data presented here, sMLV lipoplexes should tend to exist as single phase systems over a relatively large range of mixing lipid/DNA ratios (Fig. 3) and to have final (+/−) ratios that increase proportionally with the mixing (+/−) ratios (Fig. 4). Because multiple DNA copies bind to each liposome, our model also predicts that the size of sMLV lipoplexes should be comparable to that of the original liposomes, a fact that is experimentally shown by dynamic light scattering (Fig. 7).

For LUV lipoplexes, the situation is intermediate between that of sMLV and SUV lipoplexes (Fig. 9 *c*). LUV are capable of binding more than one plasmid, and for the lowest

mixing (+/−) ratios, LUV will bind multiple plasmids (*bottom left panel*). As the mixing (+/−) ratio increases to intermediate values, the number of plasmids per vesicle will decline, but all vesicles will still bind DNA (*bottom middle panel*). Therefore, to this point, LUV behave similarly to sMLV. However, because LUV are much smaller than sMLV, the number of plasmids per liposome will fall below one within the range of mixing (+/−) ratios we have used. For those higher mixing (+/−) ratios, some LUV will bind a single plasmid, which will coexist with an excess of DNA-free liposomes (*bottom right panel*). Whether the events that occur subsequent to initial binding depicted here will involve some or all of the DNA-free liposomes is unclear. However, once the lipoplexes are assembled, they will carry a net positive charge, and the unbound liposomes are expected to be repelled from the cationic lipoplexes, and to coexist as a second phase with the condensed lipoplexes. In the case of 100-nm LUV, this model accurately predicts the initial rise of the final (+/−) ratio, and the subsequent approach toward a constant final (+/−) ratio of ~4. However, the model also predicts differences in the maximal final (+/−) ratios among the three types of LUV, a fact that is not observed experimentally (Fig. 6). This suggests that either the size differences among those LUV are not sufficiently large to result in a significant difference in the point at which the maximal (+/−) ratios are achieved or that additional factors may be involved in determining those maximal ratios.

Careful interpretation of our ITC experiments provides a significant confirmation of several key aspects of the model described above. In the case of SUV, the model suggests that SUV lipoplexes will contain no more lipid than is necessary to effect complete neutralization of the DNA. Therefore, the maximal possible (+/−) ratio should correspond to the maximal capacity of the lipid for DNA binding. Revealed by the end point of the ITC titration, this value is in excellent agreement with the maximal possible final (+/−) ratio obtained in the gradient studies. In the case of sMLV, the model suggests that lipid excess to what is required to neutralize DNA is trapped in sMLV lipoplexes owing to the excess binding capacity of the liposomes at higher (+/−) ratios. However, the close dependence of mixing and final ratios suggests that such excess lipid is potentially available to bind DNA if sufficient DNA is added. ITC studies of sMLV lipoplexes confirm that this excess lipid is available to bind further DNA, and that the inherent capacity of sMLV to bind DNA is similar to that of SUV. This further agrees with the model proposed above.

Similarly to other studies that used liposomes containing DOPE in their composition (Lobo et al., 2001; Pozharski and MacDonald, 2002), our ITC data show that DOTIM/DOPE (1:1) interact with DNA through an exothermic reaction (Fig. 8). As shown by Lobo et al. (2001), this is related to the fact that the DOPE amine groups exist in the unprotonated state before DNA binding, a phenomenon that is caused by the relatively high surface pH usually measured in cationic liposomes (Zuidam and Barenholz, 1999), and to the concomitant proton uptake upon lipoplex formation.

Finally, one question regarding sMLV concerns the extent to which their lamellarity may be a factor in the observations that are described here. Multilamellarity would reduce the fraction of the lipid available on the outer surface of the liposome population for initial binding of DNA, and this might increase the (+/−) ratio in the lipoplexes. In an extreme case, the lamellarity might so limit the amount of liposomal lipid available for DNA binding that lipoplexes might coexist with a DNA excess in a region where the mixing (+/−) ratio is greater than 1. Our experiments do not support this interpretation for several reasons. First, were this correct, our gradient studies would have shown the presence of lipoplexes with high final (+/−) ratios, even for low mixing (+/−) ratios, and a free DNA fraction. Second, our ITC studies would have shown an endpoint for sMLV at a mixing (+/−) ratio that was much greater than that seen with SUV. Therefore, it seems unlikely that lamellarity, rather than liposome size, is a factor in the observations that we have made. We have used cobalt quenching of *N*-Rh-PE to determine lamellarity, and have found only a limited lamellarity for sMLV (data not shown). Based on what is known about the formation of charged liposomes in nonionic media, it is likely that sMLV formed in 5% w/v glucose will be multilamellar to only a limited extent.

In conclusion, the marked differences observed between SUV and larger liposomes in the formation of lipoplexes may be explained by a simple consideration of the effects of liposome size on the capacity of each liposome for DNA binding and the number of liposomes per mol of lipid. We hope, in future studies, to examine this further and to explore its effect on the efficiency of transfection.

E. Gonçalves was a recipient of a doctoral fellowship from the Portuguese National Science Foundation, PRAXIS XXI Program (BD/11150/97). Additional funding was provided by the School of Pharmacy, University of Wisconsin-Madison.

REFERENCES

Barron, L. G., L. S. Uyechi, and F. C. Szoka, Jr. 1999. Cationic lipids are essential for gene delivery mediated by intravenous administration of lipoplexes. *Gene Ther.* 6:1179–1183.

Bligh, E. G., and W. J. Dyer. 1959. A rapid method of total lipid extraction and purification. *Can. J. Biochem. Physiol.* 37:911–917.

Boukhnikachvili, T., O. Aguerre-Chariol, M. Airiau, S. Lesieur, M. Ollivon, and J. Vacus. 1997. Structure of in-serum transfecting DNA-cationic lipid complexes. *FEBS Lett.* 409:188–194.

Bruinsma, R. 1998. Electrostatics of DNA-cationic lipid complexes: isoelectric instability. *Eur. Phys. J. B.* 4:75–88.

deHaseth, P. L., T. M. Lohman, and M. T. Record. 1977. Nonspecific interaction of the *lac* repressor with DNA: an association reaction driven by counterion release. *Biochemistry.* 16:4783–4790.

Eastman, S. J., C. Siegel, J. Tousignant, A. E. Smith, S. H. Cheng, and R. K. Scheule. 1997. Biophysical characterization of cationic lipid: DNA complexes. *Biochim. Biophys. Acta.* 1325:41–62.

Felgner, P. L., Y. Barenholz, J. P. Behr, S. H. Cheng, P. Cullis, L. Huang, J. A. Jessee, L. Seymour, F. Szoka, A. R. Thierry, E. Wagner, and G. Wu. 1997. Nomenclature for synthetic gene delivery systems. *Hum. Gene Ther.* 8:511–512.

Felgner, J. H., R. Kumar, C. N. Sridhar, C. J. Wheeler, Y. J. Tsai, R. Border, P. Ramsey, M. Martin, and P. L. Felgner. 1994. Enhanced gene delivery and mechanism studies with a novel series of cationic lipid formulations. *J. Biol. Chem.* 269:2550–2561.

Gershon, H. R., R. Ghirlando, S. B. Guttman, and A. Minsky. 1993. Mode of formation and structural features of DNA-cationic liposome complexes used for transfection. *Biochemistry.* 32:7143–7151.

Gustafsson, J., G. Arvidson, G. Karlsson, and M. Almgren. 1995. Complexes between cationic liposomes and DNA visualized by cryo-TEM. *Biochim. Biophys. Acta.* 1235:305–312.

Harries, D., S. May, W. M. Gelbart, and A. Ben-Shaul. 1998. Structure, stability, and thermodynamics of lamellar DNA-lipid complexes. *Biophys. J.* 75:159–173.

Huebner, S., J. Battersby, R. Grimm, and G. Cvec. 1999. Lipid-DNA complex formation: reorganization and rupture of lipid vesicles in the presence of DNA as observed by cryoelectron microscopy. *Biophys. J.* 76:3158–3166.

Jang, E. H., and T. D. Heath. 1997. Effect of size of cationic liposomes on *in vitro* transfection. *Pharm. Res.* 14(Supp):S54–S55. (Abstr.)

Kennedy, M. T., E. V. Pozharski, V. A. Rakhmanova, and R. C. MacDonald. 2000. Factors governing the assembly of cationic phospholipid-DNA complexes. *Biophys. J.* 78:1620–1633.

Kikuchi, I. S., and A. M. Carmona-Ribeiro. 2000. Interactions between DNA and synthetic cationic liposomes. *J. Phys. Chem. B.* 104:2829–2835.

Koltover, I., T. Salditt, J. O. Rädler, and C. R. Safinya. 1998. An inverted hexagonal phase of cationic liposome-DNA complexes related to DNA release and delivery. *Science.* 281:78–81.

Lasic, D. D., H. Strey, M. C. A. Stuart, R. Podgornik, and P. M. Frederik. 1997. The structure of DNA-liposome complexes. *J. Am. Chem. Soc.* 119:832–833.

Liu, Y., L. C. Mounkes, H. D. Liggitt, C. S. Brown, I. Solodin, T. D. Heath, and R. J. Debs. 1997. Factors influencing the efficiency of cationic liposome-mediated intravenous gene delivery. *Nat. Biotechnol.* 15:167–173.

Lin, A. J., N. L. Slack, A. Ahmad, I. Koltover, C. X. George, C. E. Samuel, and C. R. Safinya. 2000. Structure and structure-function studies of lipid/plasmid DNA complexes. *J. Drug Target.* 8:13–27.

Lobo, B. A., A. Davis, G. Koe, J. G. Smith, and C. R. Middaugh. 2001. Isothermal titration calorimetric analysis of the interaction between cationic lipids and plasmid DNA. *Arch. Biochem. Biophys.* 386:95–105.

MacDonald, R. C., G. W. Ashley, M. M. Shida, V. A. Rakhmanova, Y. S. Tarahovsky, D. P. Pantazatos, M. T. Kennedy, E. V. Pozharski, K. A. Baker, R. D. Jones, H. S. Rosenzweig, K. L. Choi, R. Qiu, and T. J. McIntosh. 1999. Physical and biological properties of cationic triesters of phosphatidylcholine. *Biophys. J.* 77:2612–2629.

Mascotti, D. P., and T. M. Lohman. 1990. Thermodynamic extent of counterion release upon binding oligolysines to single-stranded nucleic acids. *Proc. Natl. Acad. Sci. USA.* 87:3142–3146.

Matulis, D., I. Rouzina, and V. A. Bloomfield. 2002. Thermodynamics of cationic lipid binding to DNA and DNA condensation: roles of electrostatics and hydrophobicity. *J. Am. Chem. Soc.* 124:7331–7342.

Mok, K. W. C., and P. R. Cullis. 1997. Structural and fusogenic properties of cationic liposomes in the presence of plasmid DNA. *Biophys. J.* 73:2534–2545.

Pozharski, E., and R. C. MacDonald. 2002. Thermodynamics of cationic lipid-DNA complex formation as studied by isothermal titration calorimetry. *Biophys. J.* 83:556–565.

Rädler, J. O., I. Koltover, A. Jamieson, T. Salditt, and C. R. Safinya. 1998. Structure and interfacial aspects of self-assembled cationic lipid-DNA gene carrier complexes. *Langmuir.* 14:4272–4283.

Rädler, J. O., I. Koltover, T. Salditt, and C. R. Safinya. 1997. Structure of DNA-cationic liposome complexes: DNA intercalation in multilamellar membranes in distinct interhelical packing regimes. *Science.* 275:810–814.

Ross, P. C., M. L. Hensen, R. Supabphol, and S. W. Hui. 1998. Multilamellar cationic liposomes are efficient vectors for in vitro gene transfer in serum. *J. Lipos. Res.* 8:499–520.

Ross, P. C., and S. W. Hui. 1999. Lipoplex size is a major determinant of in vitro lipofection efficiency. *Gene Ther.* 6:651–659.

Schmutz, M., D. Durand, A. Debin, Y. Palvadeau, A. Etienne, and A. R. Thierry. 1999. DNA packing in stable lipid complexes designed for gene transfer initiates DNA compaction in bacteriophage. *Proc. Natl. Acad. Sci. USA.* 96:12293–12298.

Simberg, D., D. Danino, Y. Talmon, A. Minsky, M. E. Ferrari, C. J. Wheeler, and Y. Barenholz. 2001. Phase behavior, DNA ordering, and size instability of cationic lipoplexes. *J. Biol. Chem.* 276:47453–47459.

Solodin, I., C. S. Brown, M. S. Bruno, C.-Y. Chow, E.-H. Jang, R. J. Debs, and T. D. Heath. 1995. A novel series of amphiphilic imidazolinium compounds for in vitro and in vivo gene delivery. *Biochemistry.* 34:13537–13544.

Spink, C. H., and J. B. Chaires. 1997. Thermodynamics of the binding of a cationic lipid to DNA. *J. Am. Chem. Soc.* 119:10920–10928.

Sternberg, B., F. Sorgi, and L. Huang. 1994. New structures in complex formation between DNA and cationic liposomes visualized by freeze-fracture electron microscopy. *FEBS Lett.* 356:361–366.

Wagner, K., D. Harries, S. May, J. O. Rädler, and A. Ben-Shaul. 2000. Direct evidence for counterion release upon cationic lipid-DNA condensation. *Langmuir.* 16:303–306.

Xu, Y., S.-W. Hui, P. Frederik, and F. Szoka. 1999. Physicochemical characterization and purification of cationic lipoplexes. *Biophys. J.* 77: 341–353.

Zuidam, N. J., D. Hirsch-Lerner, S. Margulies, and Y. Barenholz. 1999. Lamellarity of cationic liposomes and mode of preparation of lipoplexes affect transfection efficiency. *Biochim. Biophys. Acta.* 1419:207–220.